A Virtual Instrument for Time-Frequency Analysis of Signals with Highly Nonstationary Instantaneous Frequency

Irena Orović, Milica Orlandić, Srdjan Stanković, Zdravko Uskoković

Abstract— **The paper presents an open-source virtual instrument for time-frequency analysis. The purpose is to show the correct practical implementation, and the performance, of a number of complex algorithms, and of a practical criterion (the concentration measure) to select the proper algorithm for a given signal. The virtual instrument provides efficient solutions for signals with highly nonstationary instantaneous frequency. Despite variations of signal phase function, a high concentration can be achieved by a suitable choice of distribution form. The distribution can be chosen manually, or the instrument can perform the optimal distribution selection. Namely, a procedure for automated selection of optimal distribution order is provided. The concentration measure is employed as a selection criterion. A variety of options provides different comparisons for several distributions simultaneously. Efficiency of the proposed instrument is demonstrated on various examples. It is important to emphasize that an extensive and complex theory is implemented as a set of open-source algorithms. All the algorithms can be used "as is", or modified and upgraded (even separately) by researchers and practitioners in the field. The virtual instrument is available at http://www.tfsa.ac.me/Open_source_codes.html, or upon request to the authors.**

I. INTRODUCTION

Time-frequency analysis has been a very attractive research area in the last few decades. As a result, various time-frequency distributions have been proposed [1]-[8]. They are used in numerous practical applications in the areas of biomedical signal analysis [9], [10], radar signals [11], geosciences, communications, speech, image processing and multimedia applications [12], [13], etc. Depending on the nature of the signal phase function, different distributions are used, namely: linear (spectrogram), quadratic (the Wigner distribution [1], the distributions from the Cohen class [1], [14], [15], and the S-method [16], [17]), and higher order ones [18]-[24] (polynomial distributions, distribution with complex-lag argument, etc.). Time-frequency distributions with complex-lag argument have been introduced to provide the efficient analysis for signals with highly nonstationary instantaneous frequency (IF) [23]-[27]. An interesting solution based on the complex-lag signal argument could be achieved in the ambiguity domain [28]. By employing various kernel functions, the ambiguity domain implementation results in a class of complex-lag time-frequency distributions.

Here we propose a virtual instrument that can be used for a large class of signals, including highly nonstationary ones. The instrument includes specific solutions for monocomponent and multicomponent signals. A class of complex-lag distributions with different orders is implemented. Moreover, the concept of L-Wigner distribution [29] is extended to the L-form of complex-lag distributions. The proposed instrument can be used either to calculate each distribution separately or to compare the respective results by using different distributions. Note that the instrument for time-frequency representations based on the S-method realization has been already proposed in [30]. However, not only the S-method, but also the Cohen class can be obtained as special cases of the implemented complex-lag distributions.

IEEE Transactions on Instrumentation and Measurements, Vol. 60, No. 3, March 2011.

Furthermore, it is important to emphasize that the instrument offers an optimal distribution selection for signals with different rates of IF variations. Namely, a procedure for an automated choice of appropriate distribution order is proposed. The concentration measure is employed as a criterion that increments distribution order until an optimal IF representation is achieved.

Therefore, the proposed instrument can be observed as a complex system that includes various lower and higher order distributions, for analytic and real signals (monocomponent and multicomponent ones). It represents a consistent set of algorithms that can be interesting for researches and practitioners working in this field. The instrument is available as a completely open source code software, with a number of subroutines (functions) that can be used, modified or upgraded independently. Finally, the paper combines various theoretical approaches, describes their application and implementation within the virtual instrument, which contributes to its educational dimension as well.

The paper is organized as follows. A review of time-frequency distributions within the virtual instrument is given in Section II. Section III describes the algorithm and GUI of the instrument. Various instrument applications are presented within Section IV. Concluding remarks are given in Section V.

II. THEORETICAL BACKGROUND

A review of the time-frequency distributions implemented in the proposed virtual instrument is provided in this Section. Their basic properties, advantages, and constraints, are analyzed and compared. A procedure for optimal distribution selection is provided.

For a signal in the form $x(t) = Ae^{j\phi(t)}$, the time-frequency representation providing the energy distribution along the IF can be, generally, written as follows:

$$TFR(t,\omega) = \\ = 2\pi A^2 \delta(\omega - \phi^{'}(t)) *_{\omega} FT\left\{e^{jQ(t,\tau)}\right\} *_{\omega} W(\omega), \quad (1)$$

where the Fourier transform is denoted by FT, while $W(\omega)$ is the Fourier transform of a window. The function $Q(t,\tau)$ is called a spread factor defining the distribution spread around the IF. It contains different higher order derivatives of phase function $\phi(t)$ and depends on the time-frequency distribution. The optimal distribution for a certain signal should be concentrated along its IF with the smallest spread factor.

Spectrogram

The spectrogram (square module of the short time Fourier Transform - STFT) is the simplest and the most commonly used time-frequency representation. It is defined as:

$$SPEC(t,\omega) = |STFT(t,\omega)|^2 \\ = \left| \int_{-\infty}^{\infty} x(t+\tau) w(\tau) e^{-j\omega\tau} d\tau \right|^2, \quad (2)$$

where $w(\tau)$ is a window function. The main drawback of this representation is a trade-off between time and frequency resolution.

S-method

In order to improve distribution concentration, the S-method can be used [16]. It is defined as:

$$SM(t,\omega) = \int_{-\infty}^{\infty} P(\theta) STFT(t,\omega+\theta) \times \\ \times STFT^*(t,\omega-\theta) d\theta, \quad (3)$$

where $P(\theta)$ is a finite frequency domain window. Note that two special cases of the S-method are the spectrogram and the Wigner distribution. They are obtained for $P(\theta)$=$\pi\delta(\theta)$ and $P(\theta)$=1, respectively. The S-method combines good properties of the spectrogram and the Wigner distribution. Namely, the cross-terms are reduced or even completely removed, keeping good auto-terms concentration as in the Wigner distribution. Note that, unlike the Wigner distribution, the S-method does not require oversampling of the signal. The spread factor contains the same terms as in the case of the Wigner distribution:

$$Q(t,\tau)=\phi^{(3)}(t)\frac{\tau^3}{2^2 3!}+\phi^{(5)}(t)\frac{\tau^5}{2^4 5!}+$$

$$+\phi^{(7)}(t)\frac{\tau^7}{2^6 7!}+... \qquad (4)$$

The S-method can provide an ideal representation for linear frequency-modulated signals. However, for faster IF variations, the presence of third and higher order phase derivatives becomes significant, reducing the distribution concentration.

Time-frequency distributions with complex-lag argument

In the case of signals with highly nonstationary signal phase, concentration in the time-frequency domain depends on the rate of IF variations, as well as on the distribution order and form. Hence, to deal with signals whose IF varies fast, even within a few samples, the complex-lag distributions have been introduced [20]-[24].

The N-th order time-frequency distribution with complex-lag argument has been defined as [18]:

$$CTD_N(t,\omega)=$$

$$=\int_{-\infty}^{\infty}\prod_{i=1}^{N/2}x\left(t+\frac{\tau}{N(a_i+jb_i)}\right)^{(a_i+jb_i)}$$

$$\times x\left(t-\frac{\tau}{N(a_i+jb_i)}\right)^{-(a_i+jb_i)}e^{-j\omega\tau}d\tau. \qquad (5)$$

where N is an even number representing the distribution order. The signal with a complex-lag argument is calculated by using the signal with a real argument as follows:

$$x(t\pm(a_i+jb_i)\tau)=$$

$$=\frac{1}{2\pi}\int_{-\infty}^{\infty}X(\omega)e^{j\omega(t\pm(a_i+jb_i)\tau)}d\omega, \qquad (6)$$

where $X(\omega)$ is the Fourier transform of $x(t)$. The parameters a_i and b_i define the symmetrical complex points on the unit circle. The presence of signal terms with symmetrical points $\pm(a_i+jb_i)$ eliminates all even phase derivatives from the spread factor. By a suitable choice of distribution order, some odd phase derivatives can be removed as well. Thus, the spread factor can be significantly reduced providing high distribution concentration, as it will be shown through some special cases in the sequel.

Case 1: In the case N=2, a_1=1, b_1=0, we obtain real-lag signal terms producing a form of the Wigner distribution: $CTD_2(t,\omega)=\int_{-\infty}^{\infty}x(t+\frac{\tau}{2})x^{-1}(t-\frac{\tau}{2})e^{-j\omega\tau}d\tau$, with the spread factor defined by (4).

Case 2: For N=4 and a_1=1, b_1=0, a_2=0, b_2=1, the complex-lag distribution [14] follows:

$$CTD_4(t,\omega)=$$

$$=\int_{-\infty}^{\infty}x(t+\frac{\tau}{4})x^{-1}(t-\frac{\tau}{4})\times$$

$$\times x^{-j}(t+j\frac{\tau}{4})x^{j}(t-j\frac{\tau}{4})e^{-j\omega\tau}d\tau \qquad (7)$$

By applying the Taylor series expansion to the phase of the complex-lag moment: $x(t+\frac{\tau}{4})x^{-1}(t-\frac{\tau}{4})x^{-j}(t+j\frac{\tau}{4})x^{j}(t-j\frac{\tau}{4})=e^{j\left(\phi(t+\frac{\tau}{4})-\phi(t-\frac{\tau}{4})-j\phi(t+j\frac{\tau}{4})+j\phi(t-\frac{\tau}{4})\right)}$, the spread factor is obtained as:

$$Q(t,\tau)=\phi^{(5)}(t)\frac{\tau^5}{4^4 5!}+\phi^{(9)}(t)\frac{\tau^9}{4^8 9!}+$$

$$+\phi^{(11)}(t)\frac{\tau^{11}}{4^{10}11!}+... \qquad (8)$$

Note that the distribution (7) provides significant concentration improvement with respect to the quadratic distributions and even to the polynomial distribution[1] (of the same order N=4). For instance, the dominant term in the spread factor is of the fifth order which assures an ideal concentration for signals with polynomial phase up to the fourth-order.
The discrete form of the complex-lag distribution (7) is given by:

$$[CTD_4(n,k)=$$

[1]The spread factor for the fourth-order polynomial Wigner-Ville distribution is given by: $Q(t,\tau)=-0.327\phi^{(5)}(t)\frac{\tau^5}{5!}-0.386\phi^{(7)}(t)\frac{\tau^7}{7!}-...$

$$= \sum_{m=-N_s/2}^{N_s/2} w(m)x(n+m)x^{-1}(n-m) \times c(n,m)e^{-j\frac{2\pi}{N_s}4mk}, \quad (9)$$

where n, k and m are discrete time, frequency and lag coordinate, respectively, while N_s is the number of samples within the window w. The function $c(n,m)$ is defined as: $c(n,m) = e^{\ln\left|\frac{x(n-jm)}{x(n+jm)}\right|}$. The complex-lag distribution can be calculated as a corrected form of the Wigner distribution: $CTD_4 = 2WD(n,k) *_k FT_m\{c(n,m)\}$, where $*_k$ denotes the convolution in frequency domain.

The signal with complex-lag argument is obtained as:

$$x(n \pm jm) = = \frac{1}{N_s} \sum_{k=-N_s/2}^{N_s/2} X(k)e^{\mp\frac{2\pi}{N_s}mk}e^{j\frac{2\pi}{N_s}nk}, \quad (10)$$

where $X(k)$ is the discrete Fourier transform of $x(n)$. Thus, the signal with complex-lag argument is calculated as the inverse Fourier transform of $X(k)$exp(-2$\pi mk/N_s$). Note that in the numerical realizations, the exponential term may exceed the computer precision for large $-mk$, producing calculation errors.

Case 3: Further concentration improvement can be achieved by using the sixth-order distribution. For N=6 and (a_1,b_1,a_2,b_2,a_3,b_3)= (1,0,1/2,$\sqrt{3}$/2,-1/2,$\sqrt{3}$/2), the time-frequency distribution is defined as follows:

$$CTD_6(t,\omega) = \int_{-\infty}^{\infty} x(t+\frac{\tau}{6})x^{-1}(t-\frac{\tau}{6})\times \times \left(x(t+(\frac{1}{2}+j\frac{\sqrt{3}}{2})\frac{\tau}{6}) \times x^{-1}(t-(\frac{1}{2}+j\frac{\sqrt{3}}{2})\frac{\tau}{6}) \right)^{\frac{1}{2}-j\frac{\sqrt{3}}{2}} \times \left(x(t+(-\frac{1}{2}+j\frac{\sqrt{3}}{2})\frac{\tau}{6}) \times x^{-1}(t-(-\frac{1}{2}+j\frac{\sqrt{3}}{2})\frac{\tau}{6}) \right)^{-\frac{1}{2}-j\frac{\sqrt{3}}{2}} e^{-j\omega\tau}d\tau, \quad (11)$$

where x^{-1} denotes a signal x raised to the power -1. The spread factor for this distribution is reduced in comparison with the fourth-order distribution and it is given by:

$$Q(t,\tau) = \phi^{(7)}(t)\frac{\tau^7}{6^67!} + \phi^{(13)}(t)\frac{\tau^{13}}{6^{12}13!} + ... \quad (12)$$

Case 4: N equidistant points on the unit circle are considered. Without loss of generality the following modified form of complex-lag time-frequency distribution is defined [24]:

$$CTD_N(t,\omega) = = \int_{-\infty}^{\infty} x(t+\frac{\tau}{N})x^*(t-\frac{\tau}{N})c(t,\tau)e^{-j\omega\tau}d\tau = \frac{N}{2}WD(t,\frac{N}{2}\omega) *_\omega C(t,\omega), \quad (13)$$

where $*_\omega$ denotes the convolution in the analogue frequency domain, while: $C(t,\omega) = FT\{c(t,\tau)\}$. The complex-lag concentration function $c(t,\tau)$ of order N-2 is defined as [16], [17]:

$$c(t,\tau) = = \prod_{p=1}^{N/2-1} x^{w^*_{N,p}}\left(t+w_{N,p}\frac{\tau}{N}\right) \times x^{-w^*_{N,p}}\left(t-w_{N,p}\frac{\tau}{N}\right), \quad (14)$$

where $w_{N,p} = e^{j2\pi p/N}$. The spread factor for this form is:

$$Q(t,\tau) = \phi^{(N+1)}(t)\frac{\tau^{N+1}}{N^N(N+1)!} + + \phi^{(2N+1)}(t)\frac{\tau^{2N+1}}{N^{2N}(2N+1)!} + ... \quad (15)$$

Observe that the spread factor produced by the higher order phase derivatives can be decreased arbitrarily by an appropriate choice of N, which further leads to an arbitrarily high distribution concentration.

In practical realizations, the discrete form of (13) should be used:

$$CTD_N(n,k) =$$

$$= \sum_{m=-N_s/2}^{N_s/2-1} x(n+m)x^*(n-m) \times c(n,m)e^{-j\frac{2\pi}{N_s}Nmk}$$

$$= \sum_{l=-N_s/2}^{N_s/2-1} WD(n,k+l)CF(n,k-l), \quad (16)$$

where

$$CF(n,k) = FT\{c(n,m)\} = FT\left\{ \prod_{p=1}^{N/2-1} x^{w^*_{N,p}}(n+w_{N,p}m) \times x^{-w^*_{N,p}}(n-w_{N,p}m) \right\}.$$

The signal with complex-lag argument can be obtained in the discrete form as follows:

$$x(n \pm w_{N,p}m) = \sum_{k=-N_s/2}^{N_s/2-1} X(k)e^{j\frac{2\pi}{N_s}(n\pm w_{N,p}m)k} = \sum_{k=-N_s/2}^{N_s/2-1} X(k)e^{\mp\frac{2\pi}{N_s}wi_pmk}e^{j\frac{2\pi}{N_s}(n\pm wr_pm)k}, \quad (17)$$

with $wr_p = Re\{w_{N,p}\}$, $wi_p = Im\{w_{N,p}\}$. Note that the coordinate m is multiplied by wr_p. The influence of this term can be such that an additional oversampling (or interpolations) of the signal $x(n)$ is required.

The form (13) is suitable only for monocomponent signals. Namely, for the multicomponent signals, the distribution form $CTD_N(t,\omega) = \frac{N}{2}WD(t,\frac{N}{2}\omega)_{*\omega}C(t,\omega)$, will contain cross-terms. Thus, a more general form suitable for multicomponent signals has been introduced in [24]:

$$CTD_N(t,\omega) = \int_{-\infty}^{\infty} P(\theta)SM(t,\omega+\theta)C(t,\omega-\theta)d\theta, \quad (18)$$

where the cross-terms free S-method (SM) is used instead of the Wigner distribution. Note that the frequency window $P(\theta)$ is used to avoid the cross-terms that appear due to the convolution. Thus, it has the same purpose and effects as the frequency window in the S-method.

Furthermore, to calculate $C(t,\omega)$, the complex roots are expressed as: $w_{N,p} = wr_p + jwi_p$. Then the function $c(t,\tau)$ in (14) is calculated separately for powers wr_p and wi_p, resulting in two functions $c_{r_p}(t,\tau)$ and $c_{i_p}(t,\tau)$. Hence, for a signal with Q components, the concentration function $C(t,\omega)$ is calculated according to:

$$C(t,\omega) = \int_{-\infty}^{\infty} P(\theta)C_r(t,\omega+\theta)C_i(t,\omega-\theta)d\theta, \quad (19)$$

where: equation (20)

$$C_r(t,\omega) = FT_\tau\left\{\sum_{q=1}^{Q}\prod_{p=1}^{N/2-1} c_{r_p}(t,\tau)_q\right\} = FT_\tau\left\{\sum_{q=1}^{Q}\prod_{p=1}^{\frac{N}{2}-1} e^{jwr_p angle\left(x_q(t+w_{N,p}\frac{\tau}{N})\cdot x_q^*(t-w_{N,p}\frac{\tau}{N})\right)}\right\}$$

$$C_i(t,\omega) = FT_\tau\left\{\sum_{q=1}^{Q}\prod_{p=1}^{N/2-1} c_{i_p}(t,\tau)_q\right\} = FT_\tau\left\{\sum_{q=1}^{Q}\prod_{p=1}^{\frac{N}{2}-1} e^{-jwi_p\ln\left|x_q(t+w_{N,p}\frac{\tau}{N})\cdot x_q^*(t-w_{N,p}\frac{\tau}{N})\right|}\right\}. \quad (20)$$

In this case, the signal with a complex-lag argument is calculated by separating components using the STFT [24]:

$$x(t \pm w_{N,p}\frac{\tau}{N})_q = \int_{-Wq}^{Wq} STFT(t,\omega+\omega_q(t))e^{j(t\pm\tau\frac{w_{N,p}}{N})\omega}d\omega, \quad (21)$$

where $\omega_q(t) = \arg\left\{\max_\omega STFT(t,\omega)\right\}$ represents the position of the q-th component maximum. It is assumed that the q-th signal component is within the region $[\omega_q(t)\text{-}W_q, \omega_q(t)+W_q]$. The parameter W_q defines the width of the q-th signal component in the time-frequency plane. The cross-terms will be

avoided if the assumed component width is smaller than the distance between auto-terms.

The concentration functions $C_r(t,\omega)$ and $C_i(t,\omega)$ for the sixth-order complex-lag distribution is given by:

$$C_r(t,\omega) =$$
$$= FT_\tau\left\{\sum_{q=1}^{Q} e^{j\frac{\sqrt{3}}{2}angle\left\{x_q\left(t+\frac{\sqrt{3}+j}{2}\frac{\tau}{6}\right)x_q^*\left(t-\frac{\sqrt{3}+j}{2}\frac{\tau}{6}\right)\right\}}\right.$$
$$\left.\times\, e^{j\frac{\sqrt{3}}{2}angle\left\{x_q\left(t+\frac{\sqrt{3}-j}{2}\frac{\tau}{6}\right)x_q^*\left(t-\frac{\sqrt{3}-j}{2}\frac{\tau}{6}\right)\right\}}\right\}$$
$$C_i(t,\omega) =$$
$$= FT_\tau\left\{\sum_{q=1}^{Q} e^{-j\frac{1}{2}\ln\left|x_q\left(t+\frac{\sqrt{3}+j}{2}\frac{\tau}{6}\right)x_q^*\left(t-\frac{\sqrt{3}+j}{2}\frac{\tau}{6}\right)\right|}\right.$$
$$\left.\times\, e^{-j\frac{1}{2}\ln\left|x_q\left(t+\frac{\sqrt{3}-j}{2}\frac{\tau}{6}\right)x_q^*\left(t-\frac{\sqrt{3}-j}{2}\frac{\tau}{6}\right)\right|}\right\}. \quad (22)$$

Class of complex-lag time-frequency distributions based on the ambiguity domain realization

A class of complex-lag distributions can be defined by using the ambiguity domain. Beside the reduction of cross-terms, the ambiguity domain realization provides that the disturbances caused by the miscalculation of the signal with complex-lag argument are overcome [28]. For this kind of realization different kernels can be employed.

Two ambiguity functions are defined based on (13), [28]. The real-lag ambiguity function uses the real-lag signal moment, and it is defined by:

$$AF_{rt}(\theta,\tau) = \int_{-\infty}^{\infty} x(t+\frac{\tau}{N})x^*(t-\frac{\tau}{N})e^{-j\theta t}dt. \quad (23)$$

The complex-lag ambiguity function is defined by using the concentration function $c(t,\tau)$:

$$AF_{ct}(\theta,\tau) = \int_{-\infty}^{\infty} c(t,\tau)e^{-j\theta t}dt$$
$$= \int_{-\infty}^{\infty}\prod_{p=1}^{N/2-1} x^{w_{N,p}^*}\left(t+w_{N,p}\frac{\tau}{N}\right)$$
$$\times x^{-w_{N,p}^*}\left(t-w_{N,p}\frac{\tau}{N}e^{-j\theta t}dt\right). \quad (24)$$

The real-lag ambiguity function contains cross-terms in the case of multicomponent signals, while the complex-lag ambiguity function may contain calculation errors. These disturbances can be filtered by using the kernel function $C(\theta,\tau)$:

$$AF_{rt}^c(\theta,\tau) = C(\theta,\tau)AF_{rt}(\theta,\tau),$$
$$AF_{ct}^c(\theta,\tau) = C(\theta,\tau)AF_{ct}(\theta,\tau). \quad (25)$$

The filtered ambiguity functions $AF_{rt}^c(\theta,\tau)$ and $AF_{ct}^c(\theta,\tau)$ are further convolved within the window $P(\xi)$ to obtain the resulting ambiguity function as follows [28]:

$$AF(\theta,\tau) =$$
$$= \int_{-\infty}^{\infty}\int_{-\infty}^{\infty}\int_{-\infty}^{\infty} P(\xi)e^{-j\xi\tau_1}e^{j\xi(\tau-\tau_1)}\times$$
$$\times AF_{rt}^c(\theta_1,\tau_1)AF_{ct}^c(\theta-\theta_1,\tau-\tau_1)d\tau_1 d\theta_1 d\xi. \quad (26)$$

Finally, the class of complex-lag time-frequency distributions is given by:

$$CTD_{AF}(t,\omega) =$$
$$= \frac{1}{2\pi}\int_{-\infty}^{\infty}\int_{-\infty}^{\infty} AF(\theta,\tau)e^{j\theta t-j\omega\tau}d\tau d\theta. \quad (27)$$

The distributions properties will depend on the properties of the kernel $C(\theta,\tau)$. The Gaussian, Choi-Williams, Cone, and Sinc kernels are used in this instrument.

Note that this class of time-frequency distributions contains a number of subclasses that are assigned to each specific value of order N. Thus, for example, for N=2, the resulting ambiguity function reduces to real-lag ambiguity function, and the Cohen class of quadratic distributions could be obtained. The higher order subclasses are provided for N=4, 6, etc.

The L-form of complex-lag time-frequency distributions

As one may conclude, concentration is improved by increasing distribution order but at the expense of increased computational complexity. Alternatively, the L-form of distributions can improve concentration. The L-form

of the N-th order complex-lag distribution is given by [25]:

$$CTD_N^L(t,\omega) =$$

$$=\int_{-\infty}^{\infty}\prod_{i=1}^{N/2} x\left(t+\frac{\tau}{LN(a_i+jb_i)}\right)^{\pm L(a_i+jb_i)} e^{-j\omega\tau}d\tau. \quad (28)$$

For equidistant points on the unit circle: $(a_i+jb_i)=e^{j2\pi k/N}$, $k=0,1,...,N-1$, the corresponding spread factor for the L-form is given by:

$$Q(t,\tau)=\phi^{(N+1)}(t)\frac{\tau^{N+1}}{L^N N^N(N+1)!}+$$

$$+\phi^{(2N+1)}(t)\frac{\tau^{2N+1}}{L^{2N}N^{2N}(2N+1)!}+... \quad (29)$$

Thus, each term in the spread factor will be additionally reduced. The L-form can be easily calculated by using the recursive realization as follows:

$$CTD_N^L(t,\omega) =$$

$$=\int_{-\infty}^{\infty} CTD_N^{L/2}(t,\omega+\theta)CTD_N^{L/2}(t,\omega-\theta)d\theta, \quad (30)$$

and it can be used for each of the distribution forms defined by equations (13), (18), and (27). For example, for L=2, it represents a simple convolution of the basic distribution form $GCD_N(t,\omega)$.

A. Optimal distribution selection

The choice of distribution form will depend on the nature of signal's IF. Namely, faster IF variations require higher distribution order. Thus, in the case of analytical signals, the appropriate form of distribution can be chosen according to the mean squared error (MSE) of the IF estimation:

$$MSE=\frac{1}{N}\sum(f(t)-\hat{f}(t))^2 < MSE_0. \quad (31)$$

The lowest order distribution providing an MSE that is smaller than the predefined value MSE_0 will be chosen. Note that $f(t)$ denotes the exact IF, while the estimated $\hat{f}(t)$ is: $\hat{f}(t)=\arg\max_{\omega}\{CTD(t,\omega)\}$. However, in the case of real signals, the exact IF is usually unknown. Thus, an alternative solution for distribution selection can be provided by using the concentration measure [31]-[33]. A simple concentration measure can be defined as [33]:

$$M_N=\frac{\int_{-\infty}^{\infty}\int_{-\infty}^{\infty}|TFD_N(t,\omega)|^4\,d\omega d\tau}{\left(\int_{-\infty}^{\infty}\int_{-\infty}^{\infty}|TFD_N(t,\omega)|^2\,d\omega d\tau\right)^2}, \quad (32)$$

where TFD_N denotes the N-th order time-frequency distribution. The optimal distribution selection is performed through the following steps:

1. The concentration measure M_2 is calculated for N=2, i.e., for the Wigner distribution;
2. If $M_N \geq M_0$, the N-th order distribution is an optimal choice.
3. If $M_N < M_0$, set N=N+2;
4. Calculate M_N and go to step 2.

Therefore, the lowest order distribution satisfying $M_N \geq M_0$ will be chosen as the optimal one. The threshold value M_0 is obtained experimentally. Namely, a set of test signals is considered. For all of them, the different order time-frequency distributions are calculated (for N=2,4,6,...). Furthermore, for each test signal, an optimal distribution is chosen as the lowest Nth-order distribution providing satisfactory IF representation. Then, the concentration measures for the chosen distributions are used to define M_0: $M_0 = \min(M_{N_1}^1,...,M_{N_i}^i,..,M_{N_S}^S)$, where i indicates the i-th signal, while S is the number of test signals.

III. Virtual Instrument Description

A user-friendly virtual instrument for the time-frequency analysis is presented in this Section. The proposed virtual instrument is implemented in Matlab 7. The outlook of the instrument is shown in Fig. 1. The instrument source code is available at http://www.tfsa.ac.me/Open_source_codes.html.

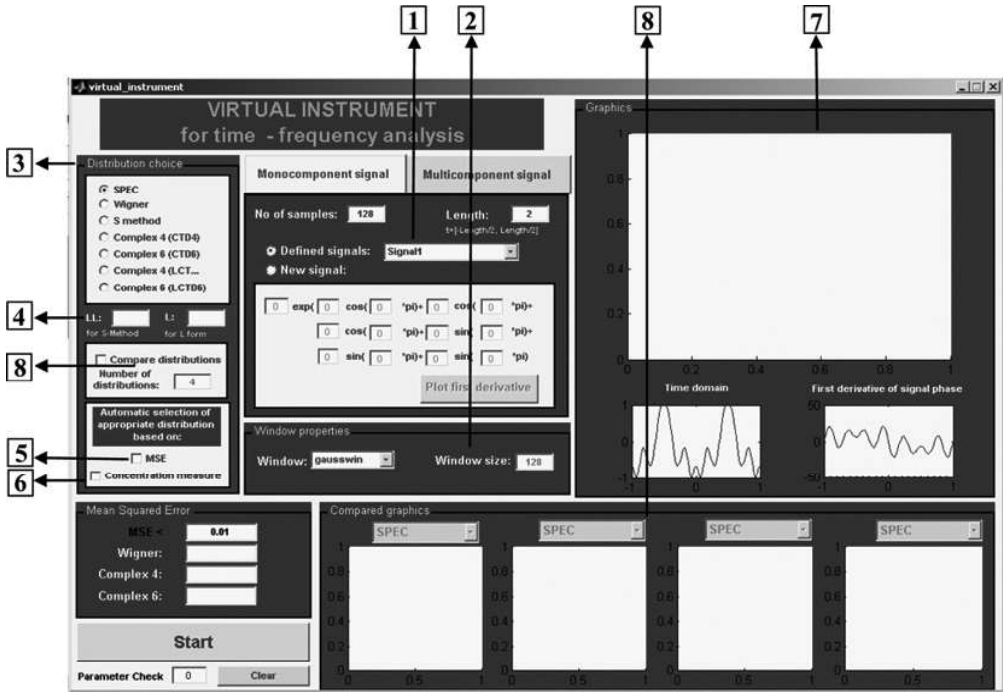

Fig. 1. The outlook of the proposed virtual instrument

The following time-frequency distributions are included, namely: the spectrogram, the Wigner distribution, the S-method, the complex-lag distributions of various orders, the class of ambiguity domain based complex-lag distribution including the Cohen class, as well as the L-forms of distributions. The instrument provides realizations for both monocomponent and multicomponent signals. Some of the input and output fields and panels, enumerated in Fig. 1, are described in the sequel.

1. Input signal: The input signal can be chosen from the list of *Defined signals* where several illustrative examples are offered. Otherwise, for an arbitrarily signal with nonlinear phase function in the form:

$$f(t) = \\ = A\, e^{a_1 \cos(b_1 \pi t) + a_2 \cos(b_2 \pi t) + a_3 \cos(b_3 \pi t)} \\ \times e^{a_4 \sin(b_4 \pi t) + a_5 \sin(b_5 \pi t) + a_6 \sin(b_6 \pi t)}, \qquad (33)$$

the users should choose some real values for the parameters A, a_1, a_2, a_3, a_4, a_5, a_6, b_1, b_2, b_3, b_4, b_5, b_6. Also, the signal length should be specified.

2. Window function: Various types of the lag-window functions (rectangular, Gaussian, Hanning, Hamming) can be chosen within the **Window properties** panel.

3. Distribution choice (manually): The user can choose a distribution within the **Distribution choice** panel, where: *SPEC* is spectrogram, *Wigner* is the Wigner distribution, *S method* is the S-method, *Complex 4* stands for the fourth-order complex-lag distribution, and *Complex 6* is the sixth-order complex-lag distribution.

4. Input L for L-form of distribution: To improve concentration, the L-form can be considered for each of the above mentioned distribution, by setting L to a value greater than 1. The default value is L=1, and it corresponds to the basic distribution form. Input LL that determines the frequency window width in the S-method (the default values is 12).

5. Choose distribution according to the predefined MSE: The automated selection of ap-

propriate distribution for a considered analytic signal is done according to the MSE of IF estimation. Here, the MSE should be lower than the predefined value that is the input of the field: *MSE* <. This option is especially interesting and useful for educational purposes.
6. Choose distribution according to the concentration measure: In the case of signal with unknown phase function, the concentration measure is used instead of MSE.
7. Main plotting window: By pressing Start button, the chosen time-frequency distribution will appear in the main plotting window (axes 1). Two additional windows are also available: the first one (axes 2) is used to plot the input signal, while the second (axes 3) plots its exact IF.
8. Comparison of distributions: a comparison of different distributions is provided (**Compare distributions** option and **Compared graphics** panel in Fig. 1). First the user should select the check button *Compare distributions* and enter the number of distributions that will be compared. Further, the distributions that should be compared are selected from the drop down menu for each plot window within the panel **Compared graphics** (axes 4, axes 5, axes 6, axes 7).

The scheme of the algorithm for the proposed virtual instrument is illustrated in Fig. 2. Depending on the number of components, the algorithm performs the realization for monocomponent or multicomponent signals.

Monocomponent signal: The user enters the number of samples and/or length in seconds, as well as the lag window parameters (the window width, i.e., the number of samples within the window, and the type of window). Afterwards, if the concentration improvement is required, the parameter L should be increased to provide the L-form of a distribution. Otherwise, the basic distribution form will be calculated (L=1). Furthermore, one may select a certain distribution manually or may start the procedure for optimal distribution search. When the distribution is selected manually, there is a possibility to compare it with four additional distributions which will be displayed within the auxiliary windows (axes 4, axes 5, axes 6, axes 7) in the **Compared graphics** panel of the virtual instrument. The optimal distribution search procedure can be performed by using the MSE of IF estimation or by using the concentration measure. The procedure starts with the second order distribution form (N=2), i.e. the Wigner distribution, and iteratively increases the distribution order until a given condition is satisfied.

Multicomponent signals: In this case there are two realization possibilities. For the ambiguity domain realization, the kernel should be selected first. Thus, a whole class of distributions is available in this case. The L-form can be optionally used. The distribution selection procedure is done in the same way as for the monocomponent signal, but the distribution calculation is different, since it is performed in the ambiguity domain. On the other hand, if ambiguity domain is not selected, after the signal and window parameters are entered, the STFT is calculated to separate signal components. Afterwards, the previously described procedure follows (Fig. 2).

IV. Time-Frequency Analysis by Using the Virtual Instrument

A. Monocomponent signals

Example 1: Consider the signal:

$$x(t) = e^{j(5/2\cos(2\pi t)+\cos(6\pi t))}.$$

Four auxiliary plotting windows are used to compare the results obtained by the following: the spectrogram, the Wigner distribution, the fourth-order complex-lag distribution and the sixth-order complex-lag distribution, respectively (Fig. 3). The Gaussian window of the width N_w=128 samples is used for the calculation of each distribution. It can be seen that the distribution concentration for the spectrogram and the Wigner distributions are very low due to the enhanced inner interferences. The fourth-order complex-lag distribution provides significant improvement, while the sixth order distribution provides good concentration along the IF. The results could be even further improved by calculating the L form of the sixth-order distribution (*Order L*: 2), which

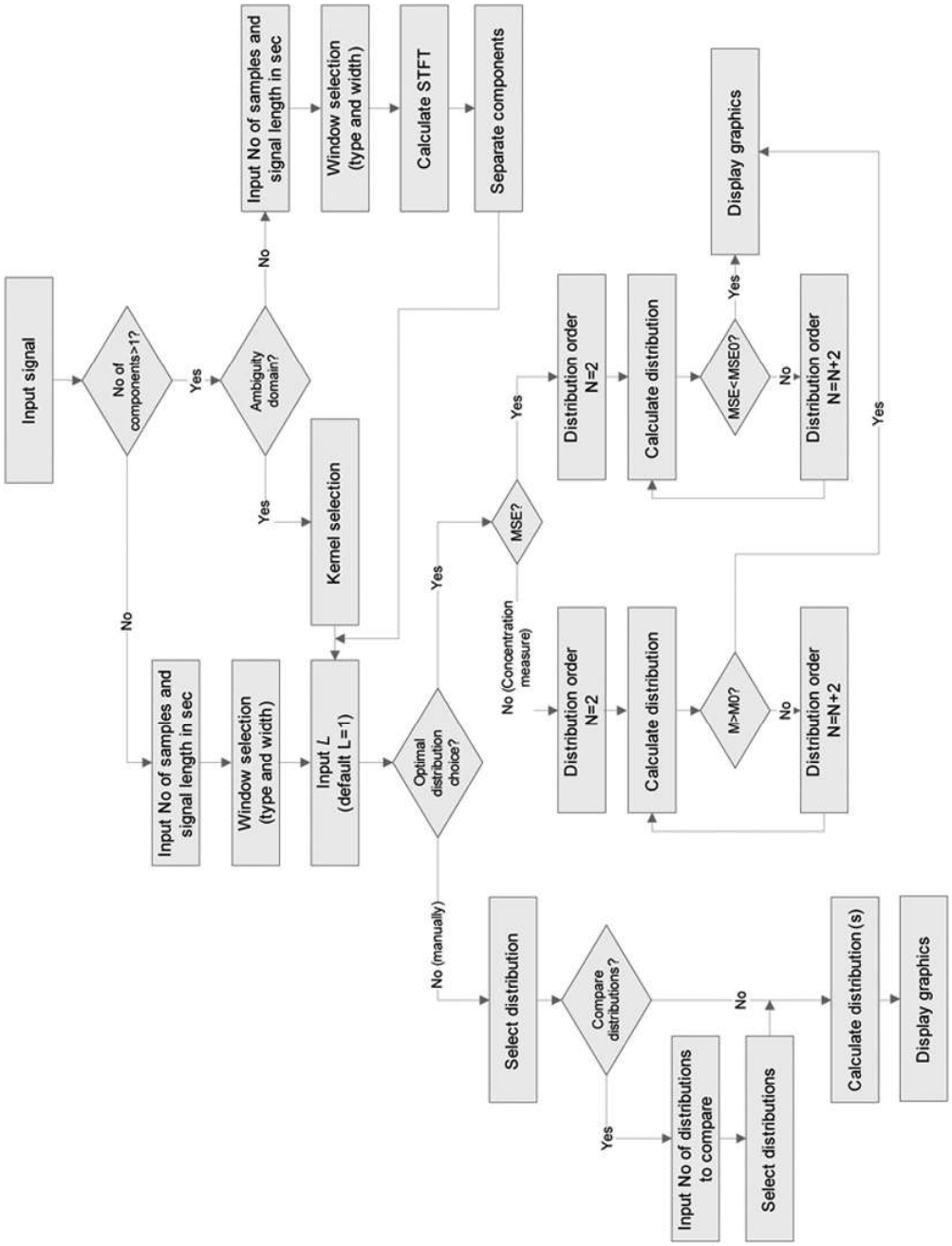

Fig. 2. The flowchart for the virtual instrument realization

is shown in the main plotting window. Note that the small disturbances within the sixth-order complex-lag distribution disappear in its L-form.

***Example 2*:** In the previous example, the suitable distribution form has been chosen manually. However, the user can set the highest tolerable MSE of the IF estimation, and the instrument will automatically choose the distribution that meets the condition. For instance, let us observe two signals:

$$y(t) = e^{j(7.5\cos(\pi t)+1/2\cos(6\pi t))},$$

$$z(t) = e^{j(2\cos(2\pi t)+1/2\cos(8\pi t)+1/2\cos(\pi t))}.$$

The highest tolerable MSE is set to the value 0.015 (the field **MSE <**). The appropriate distributions for signals $y(t)$ and $z(t)$ are given in Fig. 4.a and b, respectively. Note that, unlike the Wigner distribution, the fourth-order complex-lag distribution provides satisfactory MSE for signal $y(t)$. Thus, the fourth-order complex-lag distribution is automatically plotted in the main plotting window, while the Wigner distribution is plotted, for the purpose of comparison, in the auxiliary window (**Compared graphics** panel). For the signal with faster variations of the IF, as it is the case with $z(t)$, the sixth-order complex-lag distribution will be automatically selected and plotted in the main plotting window, Fig. 4.b. The distributions of lower order that do not provide suitable representation of IF variations are plotted in the auxiliary windows (**Compared graphics** panel).

***Example 3*:** The mean square error (MSE) can be used only for analytic signals. Thus, a more efficient distribution selection criterion is obtained by using the concentration measure. The concentration measure M_N , (32), is calculated for different distribution orders N and for a set of test signals. The results are given in Table I (all values should be multiplied by 10^{-4}). It has been shown experimentally that for the observed set of signals, the measure $M_N > 7 \cdot 10^{-4}$ indicates a satisfactory concentration in the time-frequency plane and an efficient IF representation. Several examples, included within the instrument, are illustrated in Fig. 5. The distribution with the lowest N satisfying the criterion: $M_N > 7 \cdot 10^{-4}$ will be selected as an optimal distribution for the observed signal (shaded fields in Table I).

B. Multicomponent signals

Example 1: In this example we observe a multicomponent signal in the form:

$$s(t) = e^{4j\cos(0.5\pi t)+\frac{2}{3}\cos(5\pi t)-6.5\pi t}$$

$$+e^{4j\cos(\frac{1}{2}\pi t)+\frac{3}{2}\cos(\frac{1}{2}\pi t)+\frac{1}{2}\cos(5\pi t)+8.5\pi t},$$

which consists of two non-overlapping signals, both with fast varying phase functions. The number of samples used for the STFT calculation is N_w=128. A comparison of the Wigner distribution, the fourth and the sixth-order complex-lag distributions are given in Fig. 6 (auxiliary windows). Note that the Wigner distribution is useless since it contains emphatic cross-terms.

The fourth-order complex-lag distribution provides satisfying concentration that is further improved by using the sixth-order complex-lag distribution.

Example 2: The proposed instrument allows one to upload signals from a file. An illustration for a real musical signal is given in Fig. 7 (input option **Upload a signal**). The real musical signal with fast varying IF is considered. The fourth-order complex-lag distribution is calculated by using the ambiguity domain approach, where the Gaussian kernel is applied (main plotting window in Fig. 7).

Additionally, the fourth-order ambiguity domain based complex-lag distribution is compared with the Wigner distribution filtered by the same Gaussian kernel.

Example 3: The use of the instrument in speech and biomedical (ECG) signals analysis is illustrated in this example. Since speech contains a large number of components, the optimal time-frequency representation is obtained by using the S-method, plotted in the main window, Fig. 8. Although the spectrogram, as the simplest choice, is commonly used for speech analysis, the S-method provides significant resolution improvement with slightly higher calculation complexity. The comparison of results is given within the **Compared graphics** panel. Similarly, the results

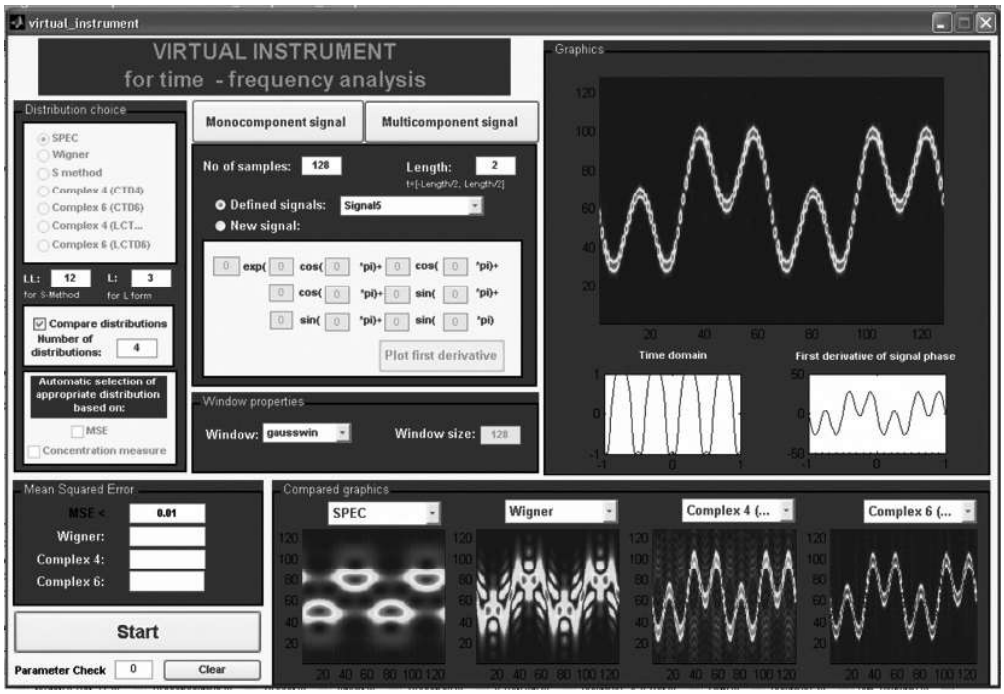

Fig. 3. Comparison of different time-frequency distributions

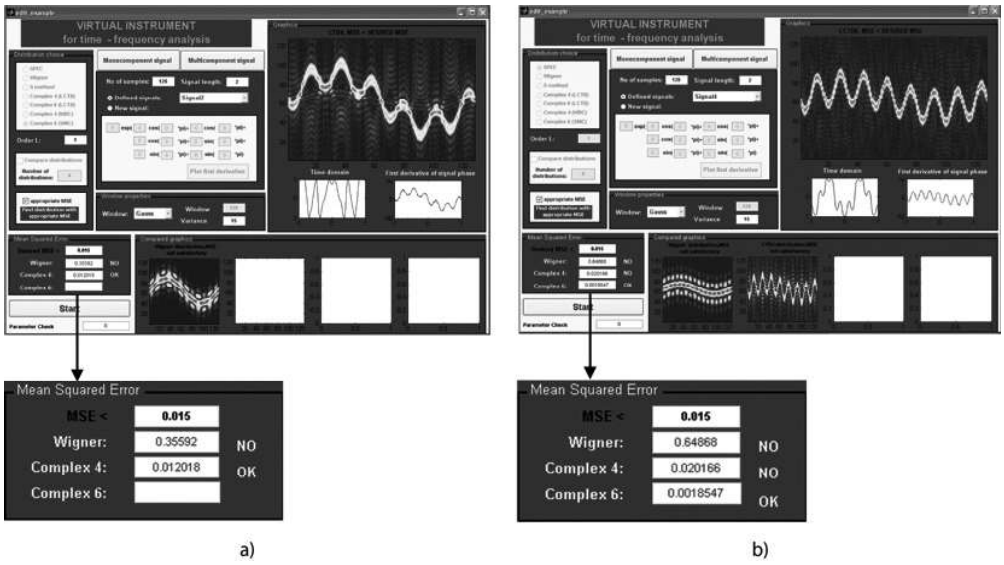

a) b)

Fig. 4. Automatic selection of appropriate time-frequency distribution a) the fourth-order complex-lag distribution, b) the sixth-order time-frequency distribution

TABLE I
MEASURES OF CONCENRATION FOR DIFFERENT SIGNALS AND DIFFERENT ORDER N

CONCENTRATION MEASURE M_N			
Signal	**WD (N=2)**	**CTD4 (N=4)**	**CTD6 (N=6)**
1	**4,4**	**4,6**	**8,62**
2	**5**	**8,26**	**13**
3	**4,31**	**7,33**	**12**
4	**3,6**	**5**	**9,96**
5	**3,23**	**4,1**	**8,17**
6	**5**	**5,85**	**11**
7	**3,93**	**4,89**	**8,3**
8	**4,98**	**8,6**	**13**
9	**6,39**	**8,86**	**13**
10	**7,3**	**8,67**	**13**

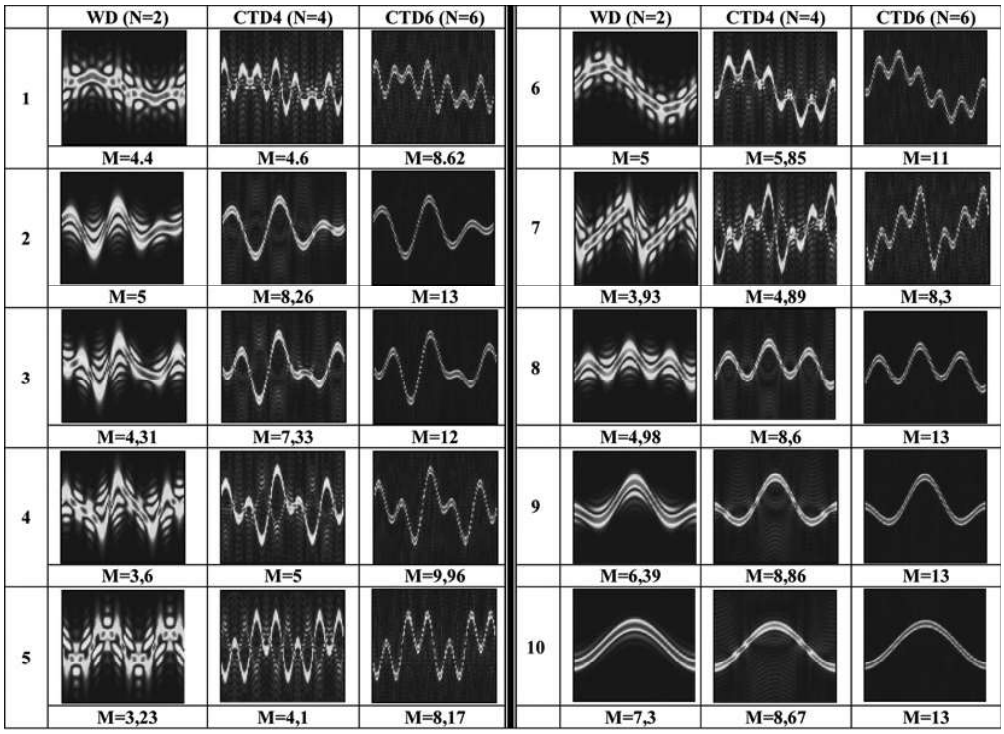

Fig. 5. Illustrations of different order distributions and corresponding concentration measures for some test signals

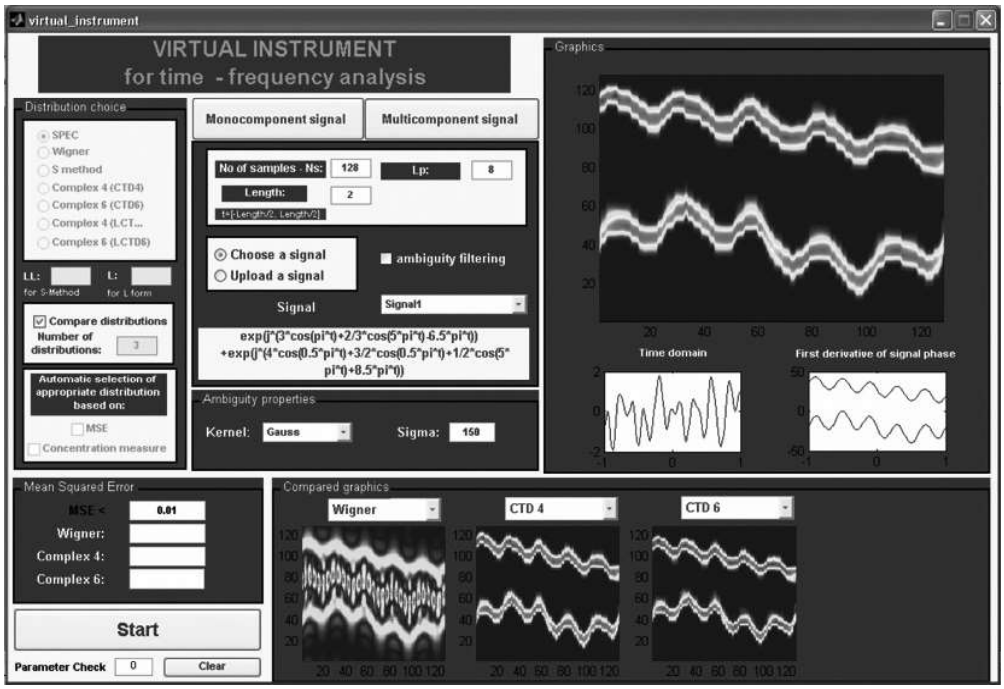

Fig. 6. Multicomponent signals analysis

for ECG signal are given in Fig. 9, where again the S-method is plotted in the main window.

V. CONCLUSION

An open-source virtual instrument for performance testing and practical implementation of several complex algorithms for nonstationary signals analysis has been presented. The instrument incorporates different Nth-order time-frequency distributions, as well as their ambiguity domain realizations. Thus, it can provide an efficient IF analysis even when it varies significantly within a few samples. Both the monocomponent and multicomponent signals realizations are considered and implemented. Additionally, the proposed virtual instrument enables a comparison of various time-frequency distributions and allows users to choose the most appropriate one for a particular signal. The selection of appropriate distribution can be done either manually or by following the optimal distribution selection procedure. Finally, it can be concluded that this instrument represents a user-friendly tool that can serve to the researchers and practitioners in the area of time-frequency signal analysis. The implemented open-source algorithms can be modified and combined with other algorithms, and thus, they could serve as a basis to construct other application-related instruments for solving specific problems.

Acknowledgment

The authors are thankful to the anonymous reviewers for their valuable comments and suggestions.

References

[1] L. Cohen, "Time-Frequency distributions-A review," *Proceedings IEEE*, Vol. 77, No. 7, pp. 941-981, July 1989.

[2] L. Cohen, *Time-Frequency analysis*, Prentice Hall, 1995.

[3] F. Hlawatsch and G.F. Boudreaux-Bartels, "Linear and Quadratic Time-Frequency Signal Representations," *IEEE Signal Processing Magazine*, Vol. 9, No. 2, pp. 21-67, Apr. 1992.

[4] M.G. Amin, W.J. Williams: "High Spectral Resolution Time-Frequency Distribution Kernels," *IEEE Trans. on Signal Processing*, Vol. 46, No. 10, pp. 2796-2804, Oct. 1998.

Fig. 7. Time-frequency analysis of real signals

[5] B. Boashash, "Estimating and interpreting the instantaneous frequency of a signal - Part 1," *IEEE Proceedings*, Vol. 80, No.4, pp. 519-538, Apr. 1992.

[6] B. Boashash, "Estimating and interpreting the instantaneous frequency of a signal - Part 2," *IEEE Proceedings*, Vol. 80, No.4, pp. 540-568, Apr. 1992.

[7] Proceedings of the IEEE, Special issue on Time-Frequency Analysis, Vol. 84, No. 9, Sept. 1996.

[8] B. Boashash, "Time-Frequency Analysis and Processing," Elsevier, 2003, Amsterdam

[9] E. Sejdic and J. Jiang, "Comparative Study of Three Time-Frequency Representations with Applications to a Novel Correlation Method," in *Proc. of IEEE International Conference on Acoustics, Speech, and Signal Processing* (ICASSP 2004), Vol. 2, Montreal, Canada, May 2004, pp. 633-636.

[10] E. Sejdic and J. Jiang, "Time-Frequency Analysis of the Heart Sounds," in *Proceedings of 2002 ECEGRS*, London, Ontario, Canada, May, 2002, pp. 5-9.

[11] Y. Zhang, M. G. Amin, and G. J. Frazer, "High-resolution time-frequency distributions for manoeuvring target detection in over-the-horizon radars," *IEE Proceedings on Radar, Sonar and Navigation*, Vol. 150, No. 4, pp. 299-304, Aug. 2003.

[12] B.G. Mobasseri, "Digital Watermarking in joint time-frequency domain," *IEEE International Conference on Image Processing*, Rochester, NY, Sept. 2002.

[13] L. Lee and S. Krishnan, "Time-frequency signal synthesis and its application in multimedia watermark detection," *EURASIP Journal on Applied Signal Processing*, Vol. 2006, Article ID 86712, 14 pages, 2006.

[14] H. Choi, W. Williams, "Improved time-frequency representation of multicomponent signals using exponential kernels," *IEEE Trans. on Acoustics and Speech*, Vol. ASSP-37, No. 6, pp. 862-871, June 1989.

[15] L.E. Atlas, Y. Zhao, R.J. Marks: "The use of cone shape kernels for generalized time-frequency representations of non-stationary signals," *IEEE Trans. on Acoustics and Speech*, Vol. 38, pp. 1084-1091, 1990.

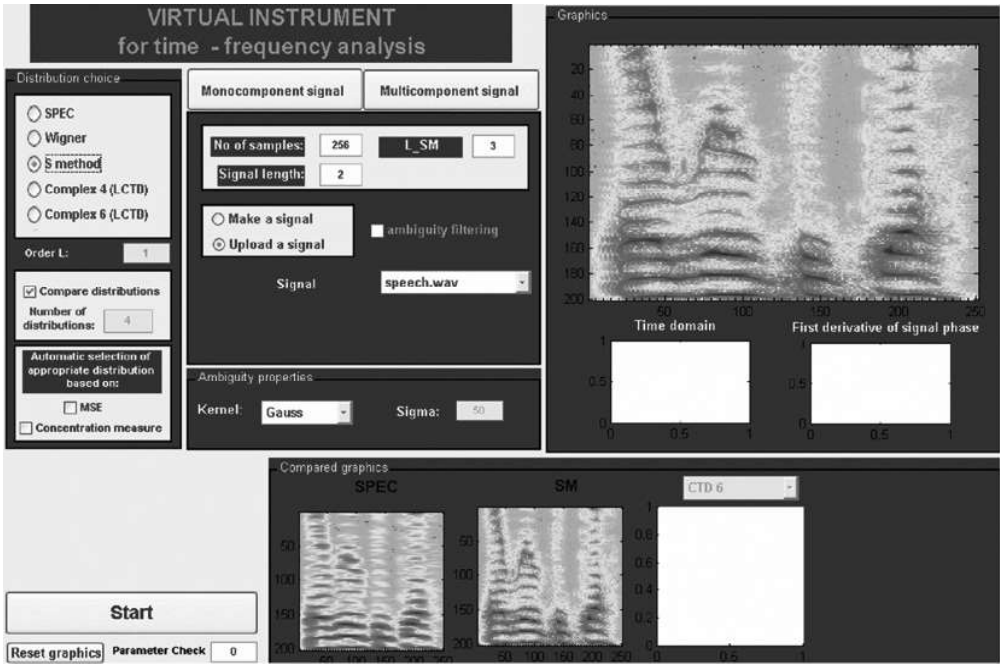

Fig. 8. Speech signal analysis by using virtual instrument

[16] LJ. Stanković, "A method for time-frequency signal analysis," *IEEE Trans. On Signal Processing*, Vol. 42, No. 1, pp.225-229, Jan. 1994.

[17] L.L. Sharf, B. Friedlander, "Toeplitz and Hankel kernels for estimating time-varying spectra of discrete-time random processes," *IEEE Trans. on Signal Processing*, Vol. 49, No. 1, pp. 179-189, Jan. 2001.

[18] B. Barkat, and B. Boashash, "Design of higher-order polynomial Wigner-Ville distributions," *IEEE Trans. on Signal Processing.*, Vol. 47, No. 9, pp. 2608-2611, Sept. 1999.

[19] B. Ristic, B. Boashash, "Relationships between the Polynomial and Higher order Wigner-Ville Distribution," *IEEE Signal Processing Letters*, Vol. 2, No. 12, pp. 227-229, Dec. 1995.

[20] S. Stanković, and LJ. Stanković, "Introducing Time-Frequency Distribution with a "Complex-Time" Argument," *Electronics Letters*, Vol. 32, No. 14, pp. 1265 - 1267, July 1996.

[21] M. Morelande, B. Senadji, B. Boashash: "Complex-lag Polynomial Wigner-Ville distribution," *in Proc. of the IEEE TENCON*, Vol. 1, Brisbane, Qld., Australia, 1997, pp. 43-46.

[22] LJ. Stanković, "Time-Frequency distributions with complex argument," *IEEE Trans. on Signal Processing*, Vol. 50, No. 3, pp. 475-486, Mar. 2002.

[23] C. Cornu, S. Stanković, C. Ioana, A. Quinquis, and LJ. Stanković, "Generalized representation derivatives for regular signals," *IEEE Trans. on Signal Processing*, Vol. 55, No. 10, pp. 4831-4838, Oct. 2007.

[24] S. Stanković, N. Žarić, I. Orović, C. Ioana, "General form of time-frequency distribution with complex-lag argument," *Electronics Letters*, Vol. 44, No. 11, pp. 699-701, May 2008.

[25] S. Stanković, I. Orović and C. Ioana, "Effects of Cauchy Integral Formula Discretization on the Precision of IF Estimation: Unified Approach to Complex-Lag Distribution and its Counterpart L-Form," *IEEE Signal Processing Letters*, Vol. 16, No. 4, pp. 327-330, Apr. 2009.

[26] I. Orović, N.Žarić, M. Orlandić, S.Stanković, "A Virtual Instrument for Highly Concentrated Time-Frequency Distributions," *ETAI* 2009, Ohrid, 2009.

[27] M. Salagean, I. Nafornita, "Time-Frequency Methods for Multicomponent Signals," *Int. Symp. on Signals, Circuits and Systems*, 2007, ISSCS 2007, vol. 1, pp.1-4.

[28] I. Orović, S. Stanković, "A Class of Highly Concentrated Time-Frequency Distributions Based on the Ambiguity Domain Representation and Complex-Lag Moment.," *EURASIP Journal on Advances in Signal Processing*, Vol. 2009., Article ID 935314, 9 pages

[29] LJ. Stanković, "A method for Improved Concentration in the Time-Frequency Analysis of Multicomponent Signals Using the L-Wigner Distribution," *IEEE Trans. on Signal Processing*, Vol. 43, No. 5, May 1995.

[30] I. Djurović, LJ. Stanković, "A Virtual Instrument for Time – Frequency Analysis", *IEEE Trans. On Instrumentation and Measurements*, Vol. 48, No. 6, Dec.1999.

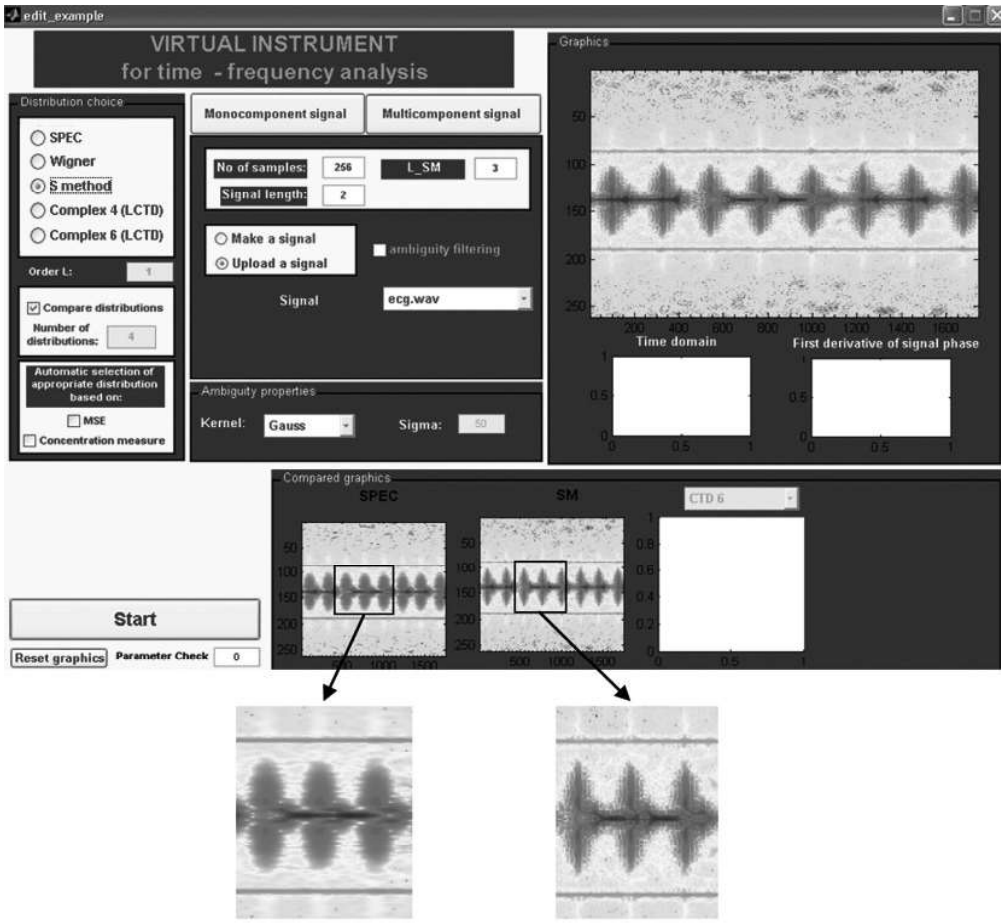

Fig. 9. Biomedical signal analysis

[31] S. Stanković, I. Đurović, R. Herpers, " Velocity and Acceleration Estimation in Video Sequences by the Local Polynomial Periodogram," *in Proc. of ISSPA*, Paris, France, 2003, Vol. 1, pp.145-148

[32] I. Shafi, J. Ahmad, S. I. Shah and F. M. Kashif, "Quantitative Evaluation of Concentrated Time-Frequency Distributions," 17^{th} *European Signal Processing Conference, EUSIPCO 2009*, August 2009, pp. 1176-1180.

[33] D.L. Jones and T.W. Parks, "A High Resolution Data-Adaptive Time-Frequency Representation," *IEEE Trans. on Acoustics, Speech and Signal Processing*, Vol. 38, No. 12, pp. 2127-2135, Dec. 1990.